The Role of Rab27a in the Regulation of Melanosome Distribution within Retinal Pigment Epithelial Cells

Clare E. Futter,* José S. Ramalho,† Gesine B. Jaissle,‡ Mathias W. Seeliger,‡ and Miguel C. Seabra§¶

*Division of Cell Biology, Institute of Ophthalmology, University College London, London EC1V 9EL, United Kingdom; †Centre of Ophthalmology, Biomedical Institute for Research in Light and Image, University of Coimbra, 3000-354 Coimbra, Portugal; ‡Department of Pathophysiology of Vision and Neuro-ophthalmology, University Eye Hospital, Tübingen, Germany; and §Cell and Molecular Biology, Division of Biomedical Sciences, Faculty of Medicine, Imperial College London, London SW7 2AZ, United Kingdom

Melanosomes within the retinal pigment epithelium (RPE) of mammals have long been thought to exhibit no movement in response to light, unlike fish and amphibian RPE. Here we show that the distribution of melanosomes within the mouse RPE undergoes modest but significant changes with the light cycle. Two hours after light onset, there is a threefold increase in the number of melanosomes in the apical processes that surround adjacent photoreceptors. In skin melanocytes, melanosomes are motile and evenly distributed throughout the cell periphery. This distribution is due to the interaction with the cortical actin cytoskeleton mediated by a tripartite complex of Rab27a, melanophilin, and myosin Va. In *ashen* (Rab27a null) mice RPE, melanosomes are unable to move beyond the adherens junction axis and do not enter apical processes, suggesting that Rab27a regulates melanosome distribution in the RPE. Unlike skin melanocytes, the effects of Rab27a are mediated through myosin VIIa in the RPE, as evidenced by the similar melanosome distribution phenotype observed in *shaker-1* mice, defective in myosin VIIa. Rab27a and myosin VIIa are likely to be required for association with and movement through the apical actin cytoskeleton, which is a prerequisite for entry into the apical processes.

INTRODUCTION

The retinal pigment epithelium (RPE) is a monolayer that lies between the photoreceptors and the choroid. RPE cells control the neural retinal environment, phagocytose the tips of photoreceptor receptor outer segments, and are required for the regeneration of visual pigment and the maintenance of the blood-retinal barrier. As the name suggests, RPE cells exhibit melanin pigment contained within the cytoplasm in membrane-enveloped granules called melanosomes. The function(s) of pigment within the RPE are not entirely clear but are likely to include absorption of stray light, thus minimizing light scatter, and the absorption of free radicals and toxins. The basal surface of the RPE contacts a basement membrane called Bruch's membrane and the choriocapillaris, a layer of fenestrated capillaries. The RPE apical surface forms numerous long processes, which reach up between the outer segments of the photoreceptors and partially envelop them. In fish and amphibians, the melanosomes of the RPE exhibit a dramatic redistribution from the cell body into the apical processes upon the onset of light, which is reversed in the dark. Melanosomes in the RPE of mammals are generally thought not to move with the light cycle (Arey, 1915; Burnside and Laties, 1979). Melanosomes

in the RPE of mammals must, however, have the ability to move as some are found within the apical processes.

In melanocytes of the skin, melanosomes move bidirectionally along microtubules and are trapped in the cell periphery by interaction with the cortical actin cytoskeleton (Wu *et al.,* 1998). This peripheral capture is essential for transfer of the granules to neighboring keratinocytes. Interaction of melanosomes with the actin cytoskeleton is mediated through a complex of Rab27a, melanophilin, and myosin Va, where Rab27a binds to the melanosome and myosin Va to actin and melanophilin is a linker between Rab27a and myosin Va (Hume *et al.,* 2001, 2002; Wu *et al.,* 2001, 2002; Fukuda *et al.,* 2002; Provance *et al.,* 2002; Strom *et al.,* 2002). Studies of the regulation of melanosome movement in melanocytes have been greatly aided by studies of melanocytes of the *ashen, leaden,* and *dilute* mice which lack functional Rab27a (Wilson *et al.,* 2000), melanophilin (Matesic *et al.,* 2001), and myosin Va (Mercer *et al.,* 1991), respectively, and are models for Griscelli syndrome in humans (Seabra *et al.,* 2002).

The melanosome dynamics within the RPE is much less well characterized. A study of the RPE of *ashen, leaden,* and *dilute* mice has not been reported. The only known phenotype has been observed in the RPE of the *shaker-1* mouse, which is defective in myosin VIIa (Gibson *et al.,* 1995). In *shaker-1* mice, the melanosomes are found exclusively in the cell body of the RPE and do not enter the apical processes (Liu *et al.,* 1998). *Shaker-1* is the mouse model for the human disease, Usher syndrome type 1B, whose patients suffer

from progressive retinal degeneration and hearing defects (Weil *et al.*, 1995; Petit, 2001). The *shaker-1* mice have hearing defects but do not suffer from retinal degeneration. Nevertheless, defects in the efficiency of degradation of phagocytosed rod outer segments (Gibbs *et al.*, 2003) and defects in opsin transport from the inner to outer segment of photoreceptors (Liu *et al.*, 1999) have been observed in *shaker-1* retinas.

That Rab27a might have a function in the RPE was suggested by its identification as a possible trigger of retinal degeneration in X-linked choroideremia, a disease characterized by slow degeneration of RPE, choroid and photoreceptors resulting in blindness at middle age (Seabra *et al.*, 1995; MacDonald *et al.*, 1998). Patients suffering from this disease lack functional REP-1, one of two REP isoforms responsible for prenylation and activation of Rab GTPases (Seabra, 1996; van den Hurk *et al.*, 1997). Although many Rabs are normally prenylated in this disease, Rab27a is not and is thus unable to associate with intracellular membranes and function properly (Seabra *et al.*, 1995; Larijani *et al.*, 2003). Rab27a appears to function through the recruitment of target proteins called effectors when it is activated upon GTP loading. Melanophilin is one such effector and forms part of a family of proteins that contain a Rab27a-binding domain (Kuroda *et al.*, 2002; Strom *et al.*, 2002). Myrip is a member of the melanophilin gene family, which has been recently identified as a binding partner of both Rab27a and myosin VIIa (El-Amraoui *et al.*, 2002). Myrip is expressed in the RPE, suggesting that melanosome movement within the RPE is regulated by interaction with the actin cytoskeleton via Rab27a-Myrip-myosin VIIa (El-Amraoui *et al.*, 2002).

In this article, we tested the hypothesis that Rab27a and myosin VIIa regulate pigment granule movement in RPE by examining the pigment granule distribution within the RPE of *ashen* and *shaker-1* mouse mutants. We have further investigated the motility of melanosomes within the RPE and investigated how Rab27a and myosin VIIa might regulate the distribution of the melanosomes within the RPE via interaction with the actin cytoskeleton.

MATERIALS AND METHODS

Materials

Biotinylated phalloidin was from Molecular Probes (Eugene, OR), rabbit antibiotin antibody from Totam Biologicals Ltd. (Peterborough, UK), protein A gold from University Medical Center (Utrecht) and rabbit anti-mouse intermediate antibody from Dako Ltd. (Ely, UK). Other primary antibodies were mouse anti-α tubulin (Kreis, 1987), anti-Rab27a mAb 4B12 and polyclonal antibody Q142 (Hume *et al.*, 2001), and antimyosin Va polyclonal antibody DB51 (Hume *et al.*, 2002); antimyosin VIIa polyclonal antibody was a gift from Steve Brown (MRC Mammalian Genetics Unit, Harwell, UK; Todorov *et al.*, 2001).

Mice

All mice were bred and maintained on 12 h-light/12 h-dark cycle under UK project license PPL 70/5071 at the Central Biomedical Services of Imperial College London or at University Eye Hospital (Tübingen). *Ashen* mice (C57BL/6J; *ash/ash*) colony was produced in the Seabra laboratory as described previously (Ramalho *et al.*, 2002). *Shaker-1* mice on a modified Balb-c background containing white-bellied agouti (A^w) mice were obtained from MRC Mammalian Genetics Unit (Harwell, UK). To maintain a colony, heterozygous females (+/*sh-1*, C/c, A^w) were bred with homozygous males (*sh-1/sh-1*, c/c, A^w). Homozygous *shaker-1* mice were albino given the linkage between both *sh-1* and *c* loci on chromosome 7. However, a spontaneous crossover event led to the generation of homozygous agouti *shaker-1* mice that were used for this study. C57BL/6 wild-type mice were purchased from B&K Universal Limited (Hull, United Kingdom).

Tissue Histology

All the mice used for histology studies were perfused with phosphate-buffered saline (pH 7.4) before dissection. Specimens were fixed in paraformal-

dehyde-glutaraldehyde fixative (4% paraformaldehyde, 5% glutaraldehyde, 0.1 M cacodylate buffer) overnight, except for the eyes, which were fixed only for 1 h. After 1 h of fixation, the eyes were cut in half and the anterior part was removed. Fixed organs were washed three times for 10 min at RT with phosphate-buffered saline. For histologic analysis, specimens were embedded in paraffin, sectioned to 3–5-μm thickness, and stained with hematoxylin and eosin.

Conventional Electron Microscopy

Mouse eyes were fixed in 1% paraformaldehyde, 3% glutaraldehyde in 0.07 M cacodylate buffer. The cornea was cut off; the lens was removed; and the eye cup was postfixed in 1% osmium 1.5% potassium ferricyanide in 0.1 M cacodylate for 2 h 4°C. After dehydrating in alcohol the eye cups were transferred to 1:1 propylene oxide:CY212 Epon and then two changes of Epon alone before embedding in Epon. Sections of 70–80 nm were stained with lead citrate before examination in a JEOL 1010 transmission electron microscope (Welwyn Garden City, United Kingdom).

Scanning Electron Microscopy

Mouse eyes were fixed in 4% paraformaldehyde in 0.1 M phosphate buffer. The cornea was cut off and the lens was removed. The neural retina was then peeled from the eyecup leaving the RPE exposed at the apical surface and still attached to Bruch's membrane on the choroid. The specimens were postfixed in 1% osmium 1.5% potassium ferricyanide in 0.1 M cacodylate and then dehydrated in alcohol. The specimens were then cut into pieces ~2-mm square and critical point dried, mounted on stubs with conductive silver paint, and sputter-coated with gold. Specimens were examined in a JEOL 6100 scanning electron microscope.

Immunofluorescence of Tissue Sections

Mouse eyes were fixed in 4% paraformaldehyde in 0.1 M phosphate buffer. The cornea was cut off and the lens was removed. The eye cup was then cut into ~3-mm squares and embedded in 10% gelatin. After allowing the gelatin to solidify at 4°C pieces of eye cup sandwiched between gelatin layers were excised and immersed for >2 h at 4°C in 2.3 M sucrose. Eye cup sandwiches were then mounted on pins and frozen in liquid nitrogen. Sections (500 nm) were cut at −80°C using a Leica FCS cryo-ultramicrotome (Milton Keynes, United Kingdom). Sections were picked up in sucrose onto slides, quenched with 0.02 M glycine, blocked with 1% BSA, and then incubated with primary antibodies, followed by fluorescent secondary antibodies and/or fluorescent phalloidin. Specimens were examined using a Bio-Rad Radiance 2000 confocal microscope (Richmond, CA).

Cryo-immunoelectron Microscopy

Mouse eyes were embedded as described for immunofluorescence above. Sections (100 nm) were cut at −120°C and picked up in 1:1 sucrose:methyl cellulose. Sections were then labeled using 10 nm protein A gold as described (Slot *et al.*, 1991). For F-actin staining sections were labeled with biotinylated phalloidin, followed by rabbit antibiotin and protein A gold. For labeling with rabbit polyclonal antibodies primary antibody was followed by protein A gold, and for labeling with mouse monoclonal antibodies primary antibody was followed by rabbit anti-mouse intermediate antibody and then protein A gold.

Electroretinography

ERGs were obtained in 12-month-old mice according to previously reported procedures. Briefly, the mice were dark-adapted overnight and anesthetized with ketamine (66.7 mg/kg) and xylazine (11.7 mg/kg). The pupils were dilated with tropicamide eye drops (Mydriatikum Stulln, Pharma Stulln, Germany). The ERG setup featured a Ganzfeld bowl, a DC amplifier, and a PC-based control and recording unit (Multiliner Vision, Jaeger/Toennies, Hoechberg, Germany). Band-pass filter cut-off frequencies were 0.1 and 3000 Hz. Single flash recordings were obtained both under dark-adapted (scotopic) and light-adapted (photopic) conditions. Light adaptation before the photopic session was performed with a background illumination of 30 cd/m² for 10 min. Single-flash stimuli were presented with increasing intensities, reaching from 10^{-4} candela second per m² (cds/m²) to 25 cds/m², divided into 10 steps of 0.5 and 1 log cds/m². Ten responses were averaged with an interstimulus interval (ISI) of either 5 or 17 s (for 1, 3, 10, 25 cd∗s/m²).

RESULTS

The Role of Rab27a in the Regulation of the Distribution of Melanosomes within the RPE

To determine whether Rab27a regulates melanosome distribution in the retina, we examined the distribution of melanosomes within the RPE of homozygous *ashen* (Rab27a null) mice, heterozygous, and wild-type mice 2 h after light onset.

A. wild type   B. *ashen*
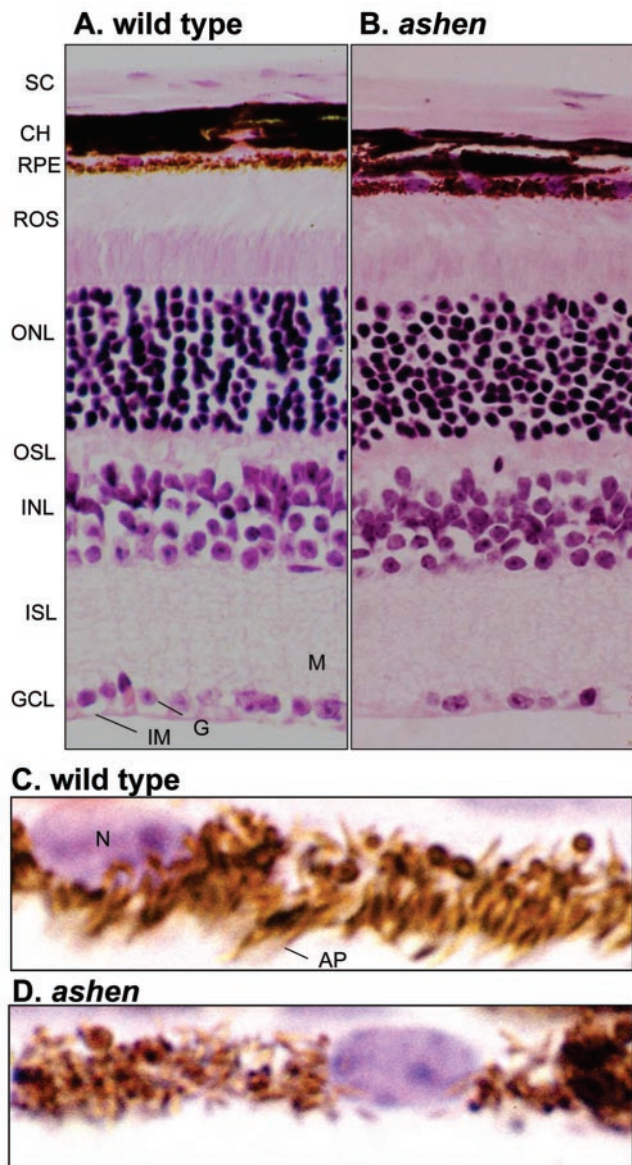
C. wild type

D. *ashen*

Figure 1. Light microscopy reveals normal organization of the retina but altered pigment granule distribution in the RPE of the *ashen* mouse. Transverse paraffin sections (3 μm) of a wild-type (A) and *ashen* mouse retina (B) at the age of 5 months stained with hematoxylin and eosin (magnification, approximately $\times$250). The bottom panels show a higher magnification of RPE from wild-type (C) and *ashen* mouse (D) (magnification, approximately $\times$1000). SC, sclera; CH, choroid; RPE, retinal pigment epithelium; ROS, photoreceptor segments of rods and cones; ONL, nuclei of rods and cones; OSL, outer synaptic layer; INL, bipolar cell nuclear layer; ISL, inner synaptic layer; GCL, ganglion cell layer; M, slender glial (Muller) cell processes; G, ganglion cells; IM, inner limiting membrane; N, RPE nucleus; AP, apical processes.

Histological sections observed under a light microscope revealed that the gross organization of the retina is normal. All retinal layers are present with normal thickness but the melanosome distribution within the *ashen* RPE is different from the wild type (Figure 1). Melanosomes in wild-type RPE are found in an area that extends clearly apical to the nucleus, whereas the distribution of melanosomes within *ashen* RPE is much more restricted in that

melanosomes are apparently absent from the area apical to the nucleus (Figure 1).

To confirm these findings, we subjected mouse retinas to thin-section electron microscopy (EM). EM analysis showed that in wild-type mice many melanosomes of the RPE are distributed within the cell body but some are found within the apical processes of the RPE interdigitating with the outer segments of photoreceptors (Figure 2A). In contrast, the melanosomes in the *ashen* retina remain in the cell body and are completely absent from the apical processes (Figure 2B). A considerable proportion of the melanosomes in the RPE of wild-type mice are elliptical in shape and oriented with their longer axis parallel to the longitudinal axis of the cell. This orientation is evident throughout the RPE cell, both above and below the adherens junctions. The melanosomes of the *ashen* mouse are more randomly oriented. Examination of multiple longitudinal sections of wild-type and *ashen* RPE indicates fewer elongated and more spherical melanosomes in *ashen* RPE. This is likely to be due to the random orientation of the melanosomes such that in thin-section more appear spherical, rather than because of a difference in melanosome shape in the *ashen* RPE. As not all apical processes of wild-type RPE contain melanosomes, changes in the distribution of melanosomes within the apical processes are most obvious in oblique sections where multiple apical processes and photoreceptor outer segments are within the same section (each RPE cells is exposed to ~40 outer segments). In these sections, it is clear that the melanosomes in homozygous *ashen* retinas do not pass beyond the level of the adherens junctions (Figure 2E), whereas in heterozygous retinas many melanosomes are seen above the level of the adherens junctions and between photoreceptor outer segments (Figure 2D).

The melanosome distribution within the *ashen* RPE mimics that of the *shaker-1* RPE (Figure 2C; Liu *et al.*, 1998) as they are also completely absent from the apical processes and show a more random orientation.

Daily Movement of Melanosomes within the RPE

Ever since the first microscopic studies of retinas over a century ago, it has been suggested that melanosome movement in mammals is minimal and very little is known about melanosome dynamics within mammalian RPE cells. The above results suggested that RPE melanosomes indeed move and that the movement may be regulated by at least two gene products, Rab27a and Myosin VIIa. To study RPE melanosome dynamics, we determined whether melanosomes of the RPE change their distribution with the daily light cycle by examining the distribution of RPE melanosomes of wild-type mice sacrificed at different times. Immediately before light onset, we observed only a small number of melanosomes in the apical processes and those are, in general, at or near the base below the outer segments (Figure 3A). Just >1 h after light onset, we observed a large number of phagosomes present in the apical cytoplasm. These phagosomes are predictably the product of light-induced phagocytosis of photoreceptor outer segments (Figure 3B). At this time point, the number of melanosomes in the apical processes remains low but the number increases significantly 1 h later. Although many of these melanosomes are still in the base of the apical processes at the 2 h after light onset time point, a significant number of melanosomes extend into the interdigitating processes (Figure 3C). At later time points (3.5 and 5.5 h after light onset), there is a gradual reduction in the number of melanosomes in the apical processes (Figure 3, D and E). Quantitation of the number of melanosomes in the apical processes at different time points
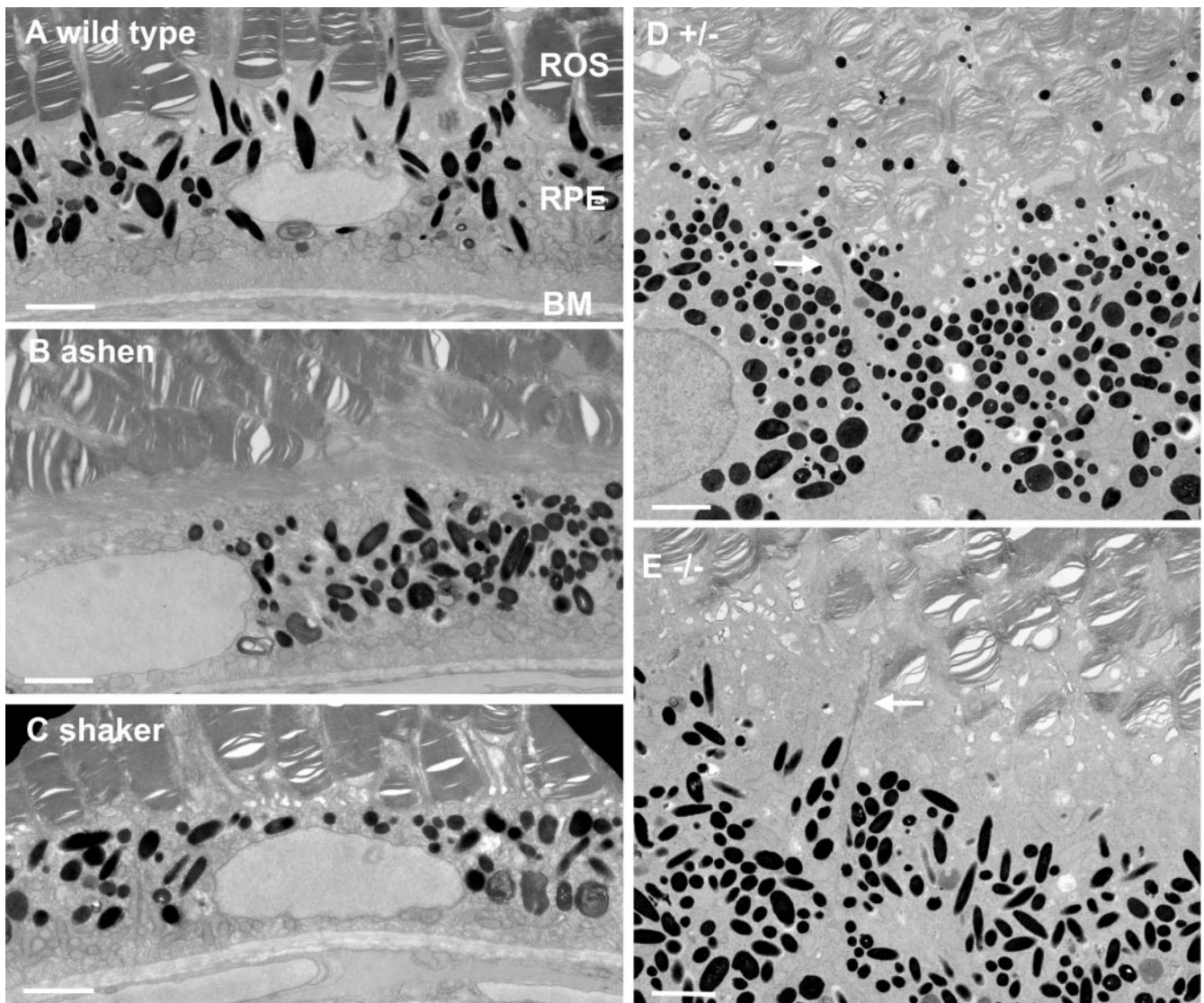
Figure 2. Electron microscopy shows that melanosomes do not move into the apical processes of RPE of *ashen* and *shaker-1* mouse. Transmission EM longitudinal sections of mouse retinas (A–C) show elongated melanosomes within the apical processes of wild-type RPE that extend between the rod outer segments (ROS), whereas in *ashen* and *shaker-1* mice melanosomes do not enter the apical processes. BM, Bruch's membrane. Oblique sections (D and E) show that many melanosomes are above the level of the adherens junctions (arrows) and extend into the apical processes between the ROS in the heterozygous (+/−, phenotypically normal) mouse (D), whereas in the homozygous (−/−) *ashen* mouse (E) the melanosomes remain below the level of the junctions. Bar, 2 μm.

indicates that there is a maximum of a threefold increase in the number of melanosomes in the apical processes 2 h after light onset, compared with the dark-adapted eye (Table 1).

Ultrastructure of the Apical Processes of Mouse RPE

Transmission EM of the wild-type mouse RPE suggested there is very little space between adjacent outer segments within which the melanosomes must move. This prompted us to examine the melanosomes within the apical processes at high magnification in order to further understand the relationship between the melanosome, the cytoskeleton, and the plasma membrane of the apical process. High magnification shows multiple very thin apical processes extending between the outer segments in the wild-type, *ashen*, and *shaker-1* RPE (Figure 4, A–C). These images suggested that the apical processes of the mutant *ashen* and *shaker-1* RPE

might be more disorganized than those of the wild-type RPE, but this is difficult to resolve by thin-section EM, where an entire apical process may not be within the section plane. It is also not possible to assess the three-dimensional organization of the apical processes by thin-section EM. We therefore performed scanning EM of the mouse RPE after removal of the photoreceptor layer. The apical processes of RPE cells are not finger-like projections but rather overlapping leaf-like projections (Figure 4, E–G). Those projections in the *ashen* and *shaker-1* RPE show no clear differences from the wild type. Although the melanosomes that enter the wild-type apical processes are elongated, their shortest diameter is still greater than the width of the apical processes when they do not contain melanosomes. When a melanosome enters an apical process, the membrane of the apical process appears to become distended around the granule
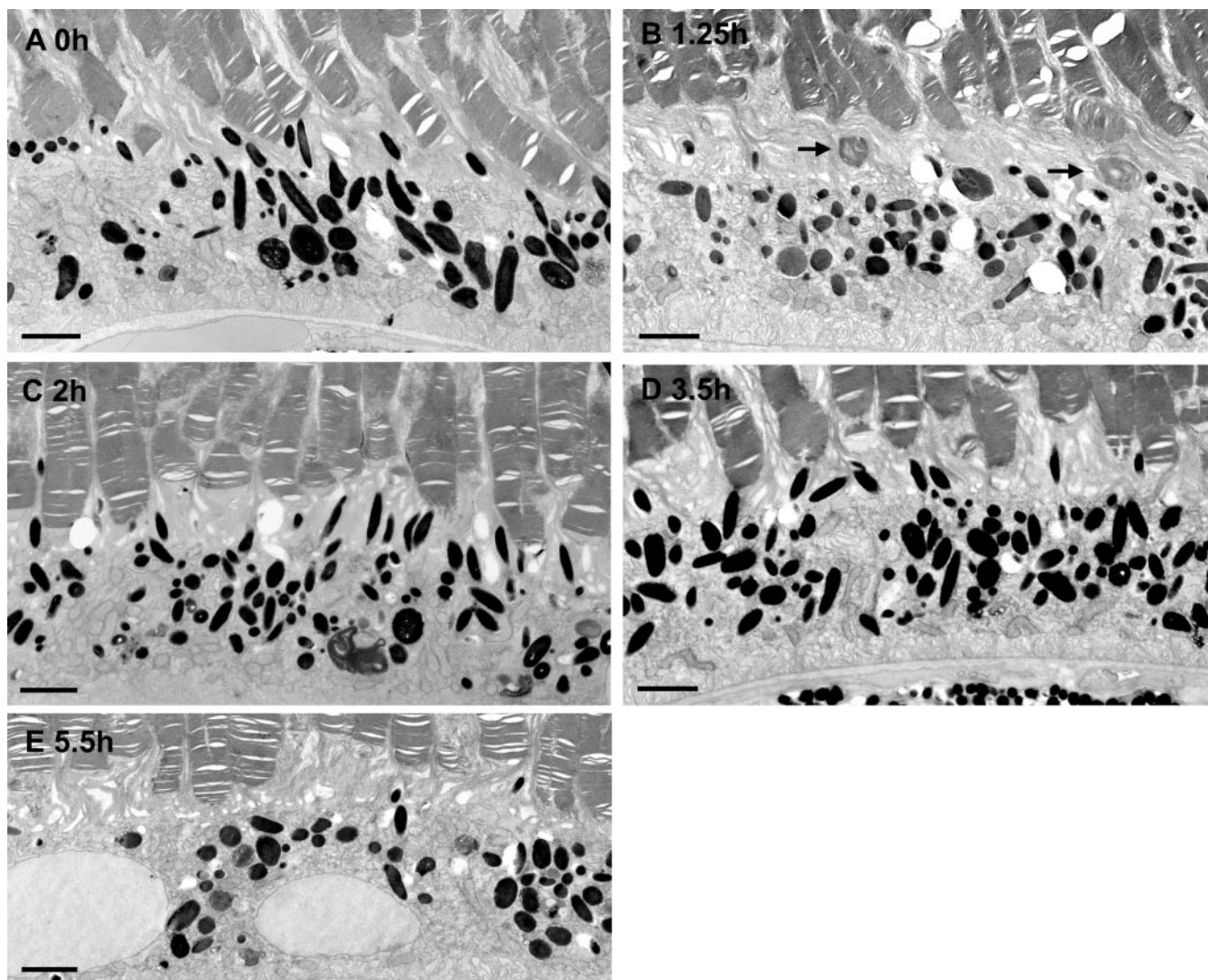
Figure 3. Daily movement of melanosomes within the RPE. 57BL/6J mice were sacrificed just before light onset (A), 1.25 h (B), 2 h (C), 3.5 h (D), and 5.5 h (E) after light onset, and longitudinal sections of RPE were examined by transmission EM. Just before light onset not many melanosomes have entered the apical processes and those that have are in the base of the process. After 1.25 h phagosomes (arrows) are visible in the apical cytoplasm, but few melanosomes are in the apical processes. After 2 h more melanosomes are in the apical processes and some have penetrated into the region between the ROS. Bar, 2 μm.

(Figure 4G). It is not possible even at the highest magnification to visualize cytoskeletal structures within the apical processes whether or not they contain melanosomes.

Interaction of Melanosomes of RPE with Cytoskeleton

Fluorescent phalloidin staining of wild-type RPE shows F-actin to be localized to the basal infoldings and to the apical processes (Figure 5, A and B). F-actin is also found in the circumferential actin ring in the apical region of the cell, which is associated with the adherens junctions. In these 0.5-μm sections that do not contain the entire cell, the circumferential actin ring appears as a short stretch of filament bundle only (Figure 5A). The apical processes are not rigid because after paraformaldehyde fixation the photoreceptors become partially or totally separated from the RPE. The RPE–photoreceptor interface is thus not as well preserved as in the conventional EM shown above, where glutaraldehyde fixation was used. Microtubules are confined to the cell body

Table 1. Quantitation of the number of melanosomes within the apical processes at different times in the light cycle

Time after light onset (h)	% melanosomes in apical processes
0	5.0
1.25	5.7
2	15.5
3.5	8.5
5.5	3.6

C57BL/6J mice were sacrificed at the indicated times after light onset and longitudinal sections of RPE examined by transmission EM. The point at which the apical process arises (which may be below the level of the outer segments) can be readily identified. Every melanosome within each section was scored for presence in the apical processes. More than 600 melanosomes were counted per time point.
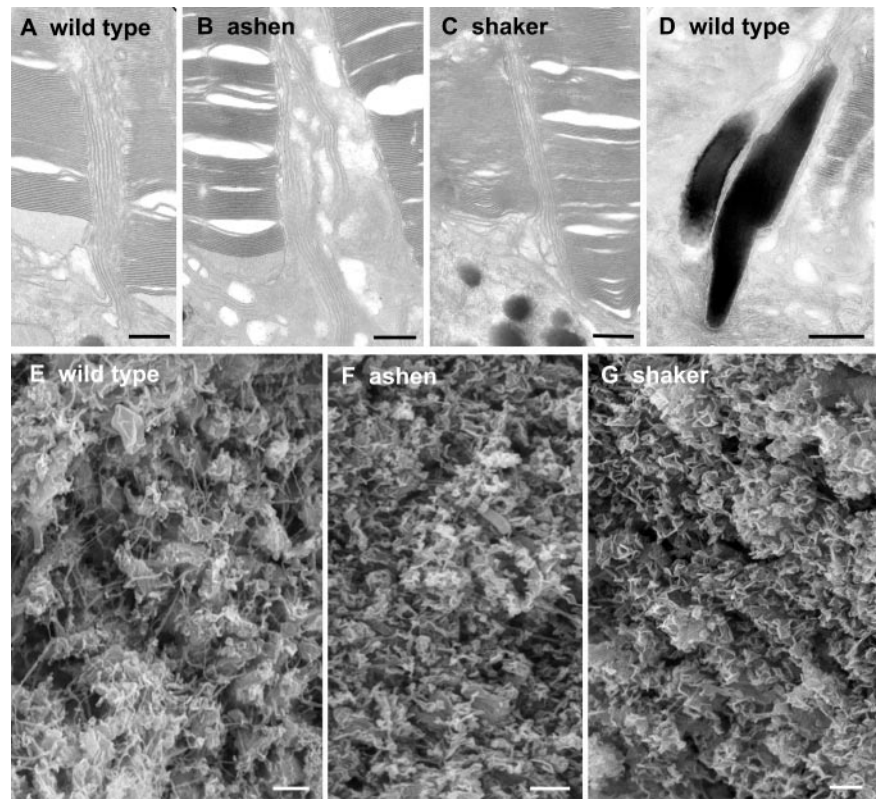
Figure 4. Ultrastructure of the apical processes of mouse RPE. Wild-type (A, D, and E), *ashen* (B and F), and *shaker-1* (C and G) RPE were processed for transmission EM (A–D) or scanning EM (E–G). Several very thin apical processes can be seen between adjacent photoreceptor outer segments in wild-type, *ashen,* and *shaker-1*. The plasma membrane of the apical process becomes distended and distorted around the pigment granule (D). Scanning EM shows that apical processes are overlapping leaf-like projections in wild-type, *ashen,* and *shaker-1*. Bar, 500 nm (A–D); 2 μm (E–G).

and absent from the apical processes. Most melanosomes are found in the microtubule-rich cell body but some have penetrated the actin-rich region of the cell, moving beyond the actin-rich cortex and into the actin-rich apical processes. Both melanosomes and actin are concentrated in the basal region of the apical processes and appear closely associated. In the *ashen* RPE, the organization of actin filaments and microtubules appears the same as the wild-type but the melanosomes are all within the microtubule-rich cell body and show no association with F-actin (Figure 5C).

Rab27a is associated with the melanosomes within the wild-type RPE, particularly with the elongated melanosomes in the apical region of the cell but also with some spherical melanosomes in the cell body (Figure 5D). Myosin VIIa stains at least some of the melanosomes in the RPE by immunofluorescence and also shows some cytoplasmic staining (Figure 5E). Some bright staining is also observed above the cell body of the RPE, which may be on outer segments of photoreceptors that have remained associated with the RPE (Figure 5E). Myosin Va shows a distribution that is very different from that of myosin VIIa. Myosin Va strongly stains structures that are clearly apical to the region containing the majority of the F-actin and melanosomes (Figure 5F). These structures (see below) are photoreceptor outer segments, which sometimes remain associated with RPE after paraformaldehyde fixation.

Cryo-immuno-EM allowed the identification of the adherens junctions and revealed F-actin labeling in the infoldings of the basal membrane (unpublished observations) and in the circumferential actin ring, just beneath the apical plasma membrane, and within the apical processes (Figure 6). Melanosomes that were at the level of or above the adherens junctions had F-actin closely associated with them, whereas those below the adherens junctions were completely devoid of actin staining. Rab27a was found on all types of melanosomes within the RPE, whether present in the cell body or in the actin-rich apical regions and whether spherical or elliptical in shape (Figure 7, A and B). Although the majority of the Rab27a staining was around the perimeter membrane of the melanosome, some Rab27a staining was observed within the lumen of the granule. Myosin VIIa staining was found on some melanosomes within the RPE. The staining was observed on both spherical and elliptical melanosomes in the cell body, both above and below the adherens junctions and within the apical processes. Nearly all the staining was present around the perimeter membrane of the melanosome (Figure 7, C–E). Myosin Va localized to the plasma membrane of photoreceptor outer segments and both the apical processes, and melanosomes were largely devoid of myosin Va staining (Figure 7, F and G).

Electroretinography Analysis of Ashen Mice

The potential impact of the lack of Rab27a on retinal function was assessed with electroretinography (ERG). Under scotopic conditions with low stimulus intensities (up to $\sim 10^{-2}$ cds/m^2), the rod system response can be determined, whereas responses of the cone system can be identified under photopic conditions. The scotopic ERG with stimulus intensities of 10^{-1} cds/m^2 and more represents a mixed response of rods and cones. Figure 8 summarizes the results obtained in *ashen* (Rab27a null) mice in comparison to wild-type controls.

A series of exemplary scotopic and photopic ERG traces obtained from an *ashen* and a wild-type control mouse is shown in Figure 8A. No significant differences in the shape of the waveforms or the size of the responses could be identified. A comparison between both groups regarding the photopic and scotopic b-wave amplitude is shown in Figure 8B. The upper and lower lines delimit the normal range (95
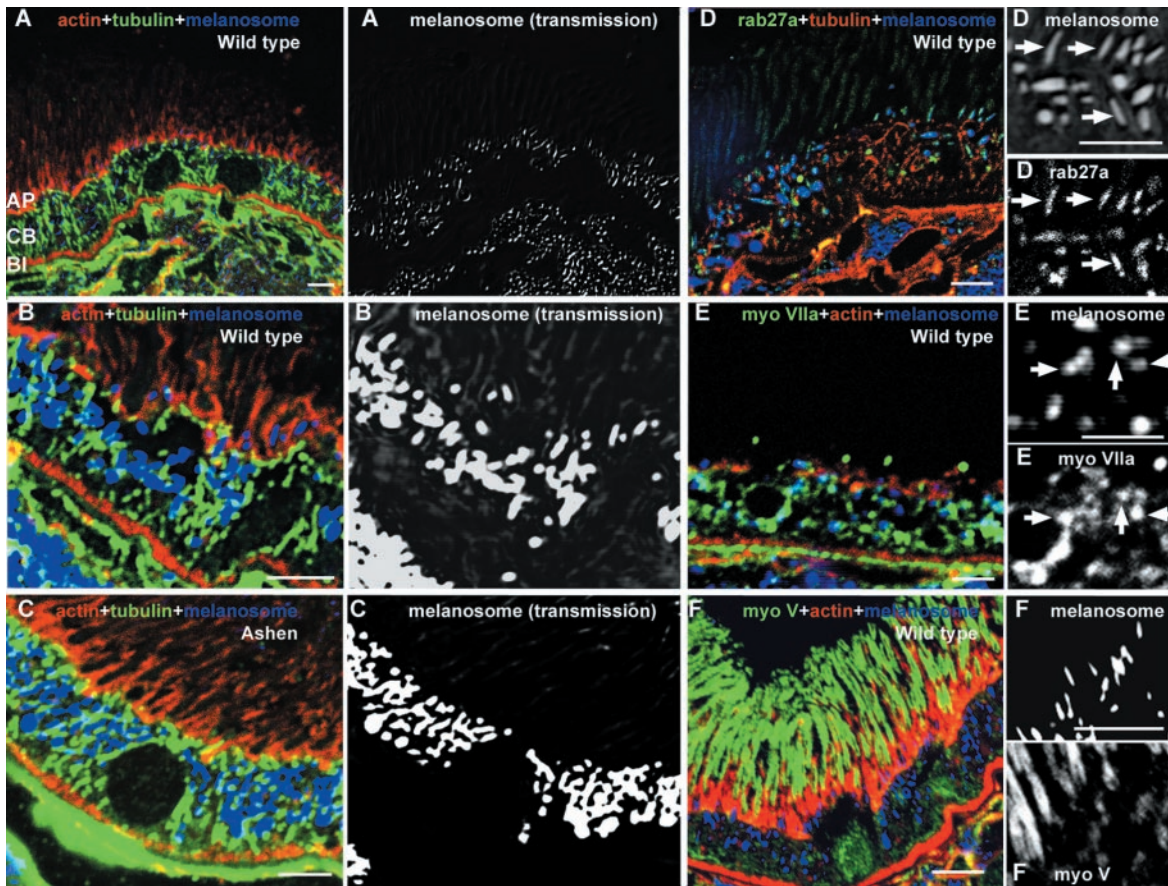
Figure 5. Immunofluorescence localization of melanosomes, Rab27a, and cytoskeletal proteins. Wild-type (A, B, and D–F) and *ashen* (C) RPE and choroid were labeled with fluorescent phalloidin (red in A–C, E, and F), antitubulin (green in A–C, red in D), anti-Rab27a (green in D), antimyosin VIIa (green in E), and antimyosin Va (green in F). Melanosomes identified by transmitted light have been artificially colored blue in the merged images. Arrows indicate examples of coincidence between melanosomes and rab27a (D) and melanosomes and myosin VIIa (E). AP, apical processes; CB, cell body; BI, basal infoldings. Bar, 5 μm.

and 5% quantiles of the control group), whereas the *ashen* data are shown as box plots (the gray boxes indicate 25 and 75% quantiles, the whiskers the 5 and 95% quantiles). The results demonstrate that the b-wave amplitude of the *ashen* mice was within normal limits for all stimulus intensities under both photopic and scotopic conditions. In summary, no functional differences between *ashen* and wild-type mice were found.

DISCUSSION

The results presented here clearly demonstrate a requirement for functional Rab27a in the light-dependent movement of melanosomes into the apical actin-rich cytoplasm and the apical processes within RPE cells. The phenotypic similarities observed in the RPE of mice lacking Rab27a or myosin VIIa suggest a model where Rab27a links melanosomes to the actin cytoskeleton via myosin VIIa to regulate melanosome distribution in the RPE.

Melanosomes in the RPE Are Not Static but Move in and out of the Very Narrow Apical Processes
Our data suggest that pigment granule distribution within the RPE is not random and that melanosomes do move in a manner which may be regulated by light. The early microscopic studies on mammalian retinas performed a century

ago suggested little, if any, movement of melanosomes, in marked contrast with amphibians and fish (reviewed in Arey, 1915; Burnside and Laties, 1979). To our knowledge, this is the first detailed description of RPE melanosome movement in mammals. The present study suggests that melanosome movements are modest, both in terms of the number of melanosomes that move at any one time and in terms of the distance that they move. The correlation between melanosome movement and the light cycle is intriguing but it remains to be determined whether light onset is the primary trigger or secondary to other light-induced changes within the photoreceptor–RPE interface. It is possible, for instance, that the light-induced phagocytosis of the tips of the photoreceptor outer segments removes physical constraints, thus allowing melanosome movement up the apical processes. As the day progresses, the outer segments move back down to a position more closely juxtaposed to the RPE and may reimpose physical constraints resulting in the gradual movement of melanosomes down the apical processes. That physical constraints exist on melanosome movement within the apical processes is suggested by the very small diameter of the apical process compared with the smallest diameter of the elongated melanosome. In summary, our observations suggest that the speed and magnitude of melanosome movement in response to light-sensitive triggers (if they exist) is slowed by physical restraints.
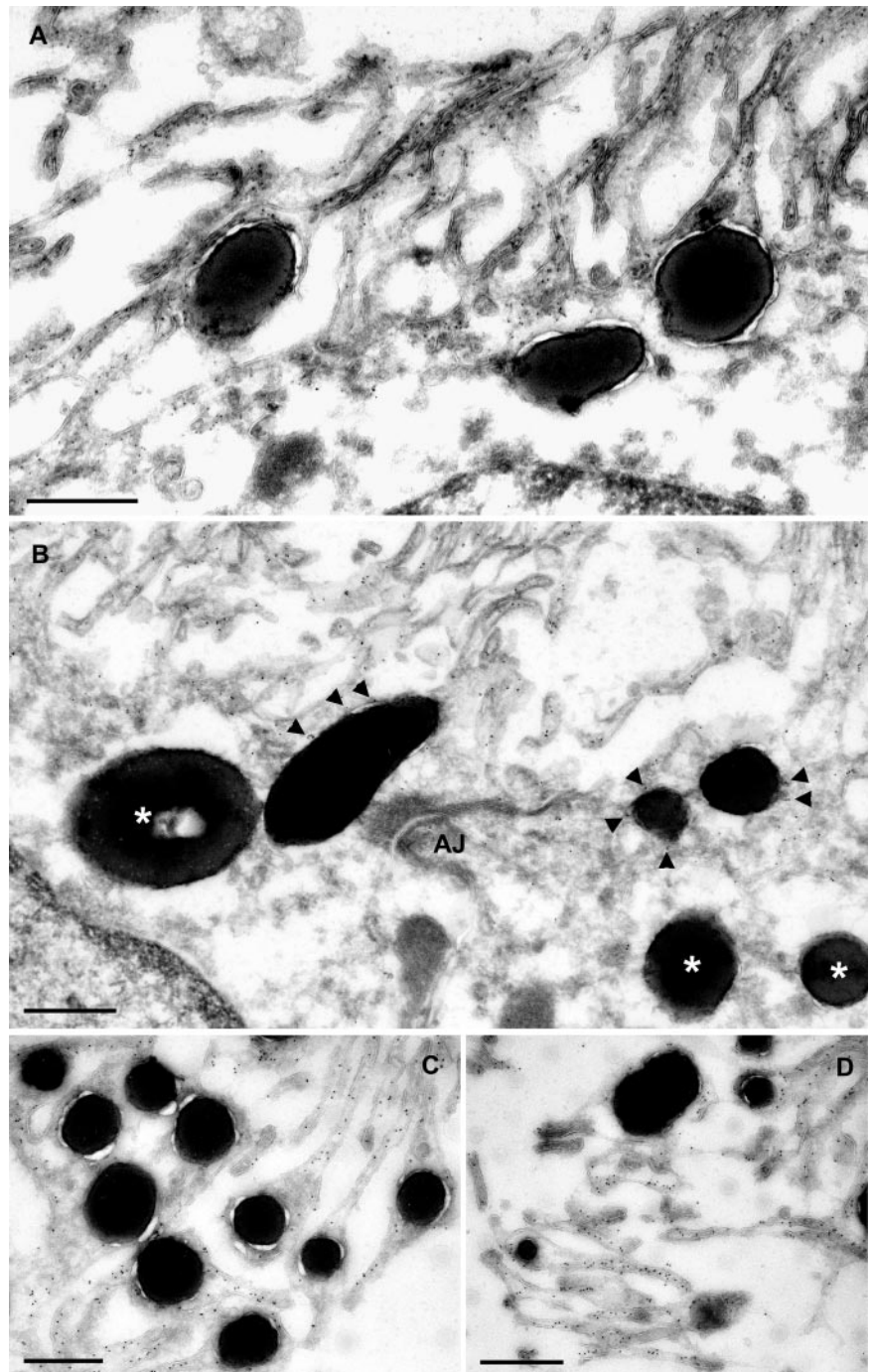
Figure 6. EM localization of melanosomes and F-actin. Cryosections of wild-type RPE were labeled with biotinylated phalloidin, antibiotin antibody and protein A gold (10 nm). Actin staining is just beneath the apical plasma membrane and within the apical processes (A). Melanosomes below the adherens junctions (AJ) are devoid of actin staining (asterisks in B), whereas those above the junctions are closely associated with F-actin staining (arrowheads in B). Oblique sections across the leaf-like processes (C and D) show the distension of the apical processes and the actin cytoskeleton within it that occurs around the pigment granule. Bar, 500 nm.

We have not been able to directly measure the kinetics of melanosome movement within mouse RPE, because pigmentation and the elaborate apical processes are not readily reproduced in cultured mammalian RPE cells.

We note that the extent and speed of melanosome movement within the RPE of some mammals may be more striking than in mice. The apical processes of the RPE of humans are more loosely packed between the photoreceptor outer segments, which may allow more movement of melanosomes within them (unpublished observations). We also show here that the apical processes of the mouse RPE are flattened leaflike, rather than fingerlike, projections, as has been reported in monkey RPE (Marmor *et al.,* 1980). Move-

ment of the melanosome within the narrow apical processes is likely to be facilitated by the fact that the apical processes are only narrow in two dimensions.

How Does Rab27a Regulate Melanosome Movement within the RPE?

In mammalian RPE cells, actin filaments are reported to be found in the infoldings of the basal plasma membrane, the lateral membrane cytoskeleton, the circumferential microfilament bundles which are associated with the adherens junctions and in the apical processes (Nguyen-Legros, 1978; Burnside and Bost-Usinger, 1998). In this study, we have
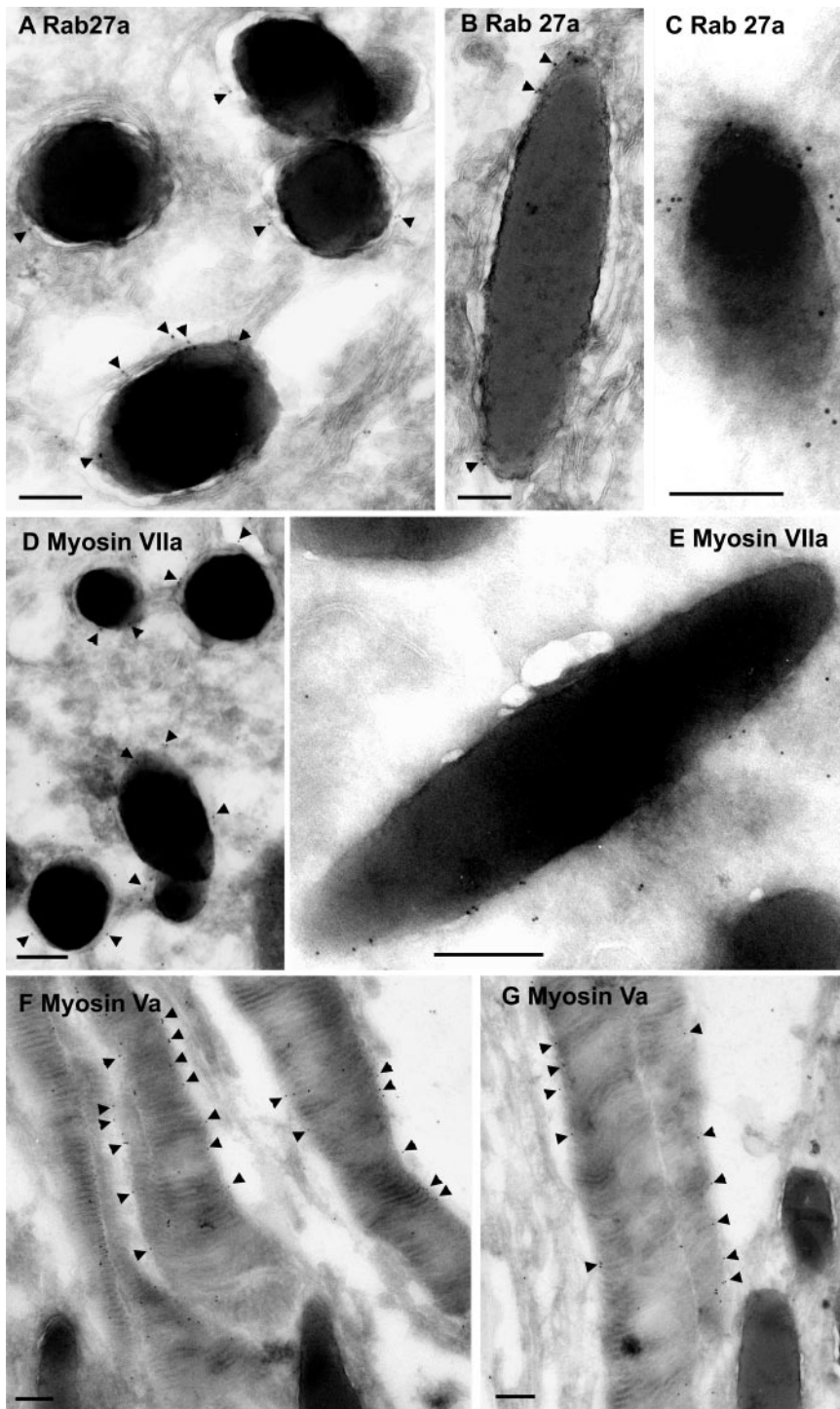
Figure 7. EM localization of Rab 27a, myosin VIIa, and myosin Va. Cryosections of wild-type RPE were labeled with 4B12 mouse anti-Rab27a (A and C), and Q142 rabbit anti-Rab27a antibody (B), anti-myosin VIIa (D and E), or anti-myosin Va (F and G). Protein A gold particles (10 nm) are indicated in the lower magnification panels by arrowheads. Rab27a is found on the perimeter membrane of most melanosomes, whether elliptical or spherical or in the cell body or the apical processes. Rab27a is also sometimes found within the lumen of the melanosome (B). Myosin VIIa is found on some melanosomes and in the cytoplasm, whereas myosin V is not found on melanosomes but strongly labels the plasma membrane of rod outer segments. Bar, 200 nm.

found F-actin in all locations but the lateral membrane cytoskeleton. F-actin was clearly visible in the basal infoldings, the circumferential microfilament bundles, beneath the apical plasma membrane and within the apical processes of mouse RPE cells (Figures 5 and 6). Microtubules were completely absent from the actin-rich apical region, including the apical processes and were found exclusively in a meshwork in the cell body.

Melanosomes in melanocytes of the skin move bidirectionally along microtubules and are trapped by a Rab27a-dependent interaction with the cortical actin cytoskeleton (Hume *et al.,* 2001; Wu *et al.,* 2001). By analogy, melanosomes in the RPE may reach the actin-rich apical region by movement along the microtubules present in the cell body, although there is no obvious alignment of melanosomes with microtubules within the cell body of the RPE.

Our observations suggest that there are no melanosomes above the level of the adherens junctions, the circumferential actin ring and the actin-rich cortex in the two mutant RPE cells presented in this study. Similar results for *shaker-1*
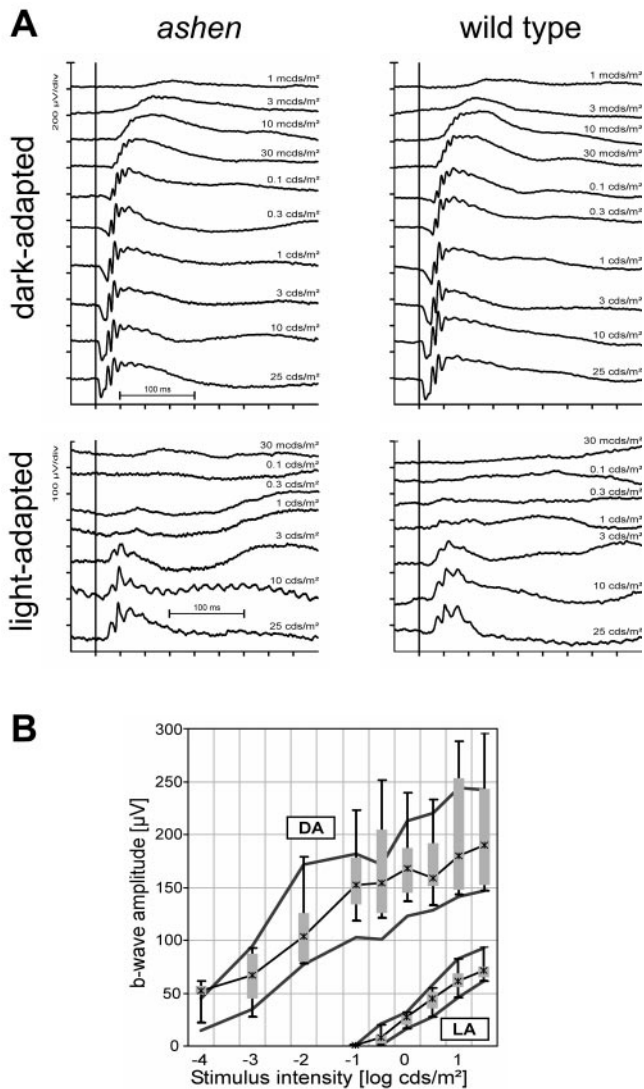
Figure 8. Electrophysiological evaluation of retinal function in *ashen* mice. (A) Representative individual traces of dark-adapted (upper row) and light-adapted (lower row) ERGs in an *ashen* mouse (left column) in comparison to control mouse (right column). Flash intensities ranged from 10^{-4} to 25 cd∗s/m². (B) Group comparison of *ashen* and wild-type mice. Displayed is the dark-adapted (DA) and light-adapted (LA) b-wave amplitude vs. the logarithm of the stimulus intensity. The response distribution characteristics of the *ashen* mice are shown as box-and-whisker-plots featuring 5 and 95% quantiles (whiskers), 25 and 75% quartiles (box), and the median (marked by an asterisk). The 5 and 95% quantiles of the control mice, indicating the normal range, are given as solid lines, revealing that the responses of the *ashen* mice were within normal limits.

retinas were previously reported (Liu *et al.*, 1998). These results suggest that Rab27a and myosin VIIa are required for association with and/or movement through the actin-ich apical region of the RPE. Both Rab27a and myosin VIIa were localized to pigment granules within the RPE, confirming the results of a previous study (El-Amraoui *et al.*, 2002). In this study we find that Rab27a and myosin VIIa are found on both spherical and elliptical melanosomes and on melanosomes found both within the microtubule-rich cell body and in the actin-rich apical regions. We have no evidence, therefore, to suggest that there are separate populations of motile

and stationary melanosomes that can be distinguished by the presence or absence of Rab27a/myosinVIIa, although we cannot rule out this possibility.

In the RPE of wild-type mice just before light onset, some of the melanosomes were found above the level of the adherens junctions in the actin-rich apical cytoplasm and a few had entered the base of the apical process. This suggests that the Rab27a-dependent association of melanosomes with apical F-actin may not be regulated by light, although subsequent movement of melanosomes up the apical processes may be light sensitive. In addition to the initial association of the melanosome with the apical actin cytoskeleton and/or movement through it, Rab27a/myosin VIIa may play a role in the subsequent movement within the apical processes. Melanosome movement along apical processes has been most extensively studied in teleost RPE, where both dispersion to the tips and aggregation within the cell body are dependent on actin filaments because they are disrupted upon cytochalasin treatment (King-Smith *et al.*, 1997). Aggregation but not dispersion may also have a requirement for microtubules (Troutt and Burnside, 1989). Unlike the apical processes of teleost RPE, those of mammals have actin filaments but no microtubules (Burnside and Laties, 1979 and this study). In mammalian RPE the actin filaments are arranged somewhat differently from those of teleost RPE or apical microvilli of other epithelial cell types in that, rather than being arranged in a central bundle they are found in parallel arrays, which may provide greater mechanical support to the leaflike projections of mammalian apical processes (Burnside and Laties, 1976). The tight packing of the apical projections between the outer segments and the distension of the apical plasma membrane and the actin filaments around the melanosome suggest that force is required for movement of the melanosome up the apical process, and it is possible that Rab27a and myosin VIIa may participate in this movement along the actin filaments.

The interaction between Rab27a and myosin VIIa is probably not direct (unpublished observations; El-Amraoui *et al.*, 2002). In skin melanocytes, Rab27a interacts indirectly with myosin Va through a bridging protein called melanophilin (Fukuda *et al.*, 2002; Strom *et al.*, 2002; Wu *et al.*, 2002). Melanophilin contains an N-terminal domain that binds activated GTP-bound Rab27a and a medial domain that binds the melanocyte-specific splice isoform of myosin Va tail. Recently, a protein related to melanophilin called Myrip (for myosin and rab interacting protein) was discovered on the basis of binding to the tail of myosin VIIa (El-Amraoui *et al.*, 2002). This protein also binds activated Rab27a and is expressed in the RPE, suggesting that it is the best candidate linker protein between Rab27a and myosin VIIa. It would be interesting to study Myrip knock-out mouse RPE, which is predicted to exhibit the same phenotype as *ashen* and *shaker-1* mice.

Possible Additional Functions of Rab27a and Myosin VIIa in the RPE

We noted in this study that the distribution of melanosomes within the microtubule-rich cell body in *ashen* and *shaker-1* mice was not substantially different from that in wild-type RPE. However, the melanosomes in the mutant cells appeared more randomly oriented both above and below the adherens junctions within the apical processes and in the cell body of the RPE. A possible mechanism whereby Rab27a would regulate granule orientation within the cell body below the adherens junctions of the RPE remains unclear because F-actin is largely absent from that area of the cell.

Myosin VIIa appears to be involved in adhesion between neighboring stereocillia of the inner ear and may play a similar role in the RPE (Self *et al.,* 1998), although we did not observe significant staining of myosin VIIa on the apical processes. It is possible that melanosome movement plays a role in the stabilization of the apical processes by unknown mechanisms. Myosin VIIa has also been implicated in the transport of phagosomes within the RPE from the apical cytoplasm to the basal cytoplasm for fusion with lysosomes (Gibbs *et al.,* 2003). We have not measured the effects of Rab27a deletion on this process, and this issue will be a focus for future studies. Furthermore, a role for melanosomes in the degradation of phagocytosed outer segments has been proposed (Thumann *et al.,* 1999). Therefore, it is possible that Rab27a and myosin VIIa regulate the motility and fusion of melanosomes and phagosomes in the RPE.

We show here that myosin Va is not found on melanosomes within the RPE but is strongly expressed on the plasma membrane of the photoreceptor outer segments. In addition, myosin Va staining was previously reported to be enriched in inner segments and rod photoreceptor synapses, suggesting that myosin V may play important roles in photoreceptor physiology (Schlamp and Williams, 1996). We observed a normal gross retinal morphology and melanosome distribution in the RPE of *dilute* mice, defective in myosin Va (unpublished observations). The strain used, *dilute-viral* exhibits a coat-color defect resulting from melanosome transport defects in skin melanocytes similar to that observed in *ashen* mice. However, the retroviral insertion in the *Myo5a* gene affects primarily the melanocyte-specific, alternative-splicing form and some myosin Va activity remains in other tissues. A more conclusive model to study would be the *dilute-lethal* strain, which is the null allele of mouse myosin Va, but unfortunately the early neonatal death of *dilute-lethal* mice hinders the examination of the RPE phenotype in these mice. As myosin Va has been clearly shown to be required for Rab27a-dependent movement of melanosomes in melanocytes of the skin, it is noteworthy that this myosin does not appear to be involved in pigment granule movement in the RPE.

Functional Consequences of Deficiency in Rab27a-dependent Movement of PGs within RPE Cells

In addition to the lack of detectable abnormalities in the ERGs of *ashen* mice, there is no evidence of retinal degeneration or visual defects (unpublished observations and Figure 8). Interestingly, the *shaker-1* mutants also do not exhibit significant visual defects or retinal degeneration, whereas human patients suffering from Usher syndrome 1B who also lack functional myosin VIIa do show such changes and undergo retinal degeneration (Libby and Steel, 2001; Petit, 2001; our unpublished observations). However, the human eye disease features a slowly progressive, gradual retinal degeneration, and vision symptoms are usually not apparent before the second decade of life. The comparatively short lifespan of the mouse may prevent the onset of retinal degeneration in the *shaker-1* model. Therefore, the failure of melanosomes to move into the apical cytoplasm/apical processes of RPE cells may contribute to gradual retinal degeneration in humans. A failure of movement of melanosomes could contribute to retinal degeneration because of reduced protection of the tips of outer segments from light damage. Alternatively, if Rab27a and myosin VIIa contribute to the phagosome maturation, this could lead to reduced photoreceptor degradation, which in turn would compromise photoreceptor function and lead to the gradual accumulation of undegraded material within the RPE, compromising its function.

This study highlights parallels and differences between melanosomes in RPE and skin melanocytes. Melanosomes of the RPE are longer lived, are frequently elliptical in shape, are not passed on to another cell type, and may be less motile, and the microtubular and actin cytoskeleton of the RPE has an organization very different from that of skin melanocytes. Future mechanistic studies on Rab27a-dependent movement of melanosomes in the different pigmented cell types should continue to contribute to a better understanding of organelle motility, intracellular form, and their pathological consequences in human disease.

REFERENCES

Arey, L.B. (1915). The occurrence and the significance of photomechanical changes in the vertebrate retina—an historical survey. J. Comp. Neurol. *25,* 535–554.

Burnside, B., and Bost-Usinger, L. (1998). The retinal pigment epithelium cytoskeleton. In: The Retinal Pigment Epithelium: Function and Disease, eds. J.F. Marmor and T.J. Wolfensberger, Oxford, UK: Oxford University Press, 41–67.

Burnside, B., and Laties, A.M. (1976). Actin filaments in apical projections of the primate pigmented epithelial cell. Invest. Ophthalmol. *15,* 570–575.

Burnside, B., and Laties, A.M. (1979). Pigment movement and cellular contractility in the retinal pigment epithelium. In: The Retinal Pigment Epithelium, eds. K.M. Zinn and M.F. Marmor, Cambridge, MA: Harvard University Press, 175–191.

El-Amraoui, A., Schonn, J.S., Kussel-Andermann, P., Blanchard, S., Desnos, C., Henry, J.P., Wolfrum, U., Darchen, F., and Petit, C. (2002). MyRIP, a novel Rab effector, enables myosin VIIa recruitment to retinal melanosomes. EMBO Rep. *3,* 463–470.

Fukuda, M., Kuroda, T.S., and Mikoshiba, K. (2002). Slac2-a/melanophilin, the missing link between Rab27 and myosin Va: implications of a tripartite protein complex for melanosome transport. J. Biol. Chem. *277,* 12432–12436.

Gibbs, D., Kitamoto, J., and Williams, D.S. (2003). Abnormal phagocytosis by retinal pigmented epithelium that lacks myosin VIIa, the Usher syndrome 1B protein. Proc. Natl. Acad. Sci. USA *100,* 6481–6486.

Gibson, F., Walsh, J., Mburu, P., Varela, A., Brown, K.A., Antonio, M., Beisel, K.W., Steel, K.P., and Brown, S.D. (1995). A type VII myosin encoded by the mouse deafness gene shaker-1. Nature *374,* 62–64.

Hume, A.N., Collinson, L.M., Hopkins, C.R., Strom, M., Barral, D.C., Bossi, G., Griffiths, G.M., and Seabra, M.C. (2002). The leaden gene product is required with Rab27a to recruit myosin Va to melanosomes in melanocytes. Traffic *3,* 193–202.

Hume, A.N., Collinson, L.M., Rapak, A., Gomes, A.Q., Hopkins, C.R., and Seabra, M.C. (2001). Rab27a regulates the peripheral distribution of melanosomes in melanocytes. J. Cell Biol. *152,* 795–808.

King-Smith, C., Paz, P., Lee, C.W., Lam, W., and Burnside, B. (1997). Bidirectional pigment granule migration in isolated retinal pigment epithelial cells requires actin but not microtubules. Cell Motil. Cytoskel. *38,* 229–249.

Kreis, T.E. (1987). Microtubules containing detyrosinated tubulin are less dynamic. EMBO J. *6,* 2597–2606.

Kuroda, T.S., Fukuda, M., Ariga, H., and Mikoshiba, K. (2002). The Slp homology domain of synaptotagmin-like proteins 1–4 and Slac2 functions as a novel Rab27A binding domain. J. Biol. Chem. *277,* 9212–9218.

Larijani, B., Hume, A.N., Tarafder, A.K., and Seabra, M.C. (2003). Multiple factors contribute to inefficient prenylation of Rab27a in Rab prenylation diseases. J. Biol. Chem. *278,* 46798–46804.

Libby, R.T., and Steel, K.P. (2001). Electroretinographic anomalies in mice with mutations in Myo7a, the gene involved in human Usher syndrome type 1B. Invest. Ophthalmol. Vis. Sci. *42,* 770–778.

Liu, X., Ondek, B., and Williams, D.S. (1998). Mutant myosin VIIa causes defective melanosome distribution in the RPE of shaker-1 mice. Nat. Genet. *19,* 117–118.

Liu, X., Udovichenko, I.P., Brown, S.D., Steel, K.P., and Williams, D.S. (1999). Myosin VIIa participates in opsin transport through the photoreceptor cilium. J. Neurosci. *19,* 6267–6274.

MacDonald, I.M., Mah, D.Y., Ho, Y.K., Lewis, R.A., and Seabra, M.C. (1998). A practical diagnostic test for choroideremia. Ophthalmology *105,* 1637–1640.

Marmor, M.F., Martin, L.J., and Tharpe, S. (1980). Osmotically induced retinal detachment in the rabbit and primate. Electron miscoscopy of the pigment epithelium. Invest. Ophthalmol. Vis. Sci. *19,* 1016–1029.

Matesic, L.E., Yip, R., Reuss, A.E., Swing, D.A., O'Sullivan, T.N., Fletcher, C.F., Copeland, N.G., and Jenkins, N.A. (2001). Mutations in Mlph, encoding a member of the Rab effector family, cause the melanosome transport defects observed in leaden mice. Proc. Natl. Acad. Sci. USA *98,* 10238–10243.

Mercer, J.A., Seperack, P.K., Strobel, M.C., Copeland, N.G., and Jenkins, N.A. (1991). Novel myosin heavy chain encoded by murine dilute coat colour locus. Nature *349,* 709–713.

Nguyen-Legros, J. (1978). Fine structure of the pigment epithelium in the vertebrate retina. Int. Rev. Cytol. Suppl. 7:287–328.

Petit, C. (2001). Usher syndrome: from genetics to pathogenesis. Annu. Rev. Genomics Hum. Genet. *2,* 271–297.

Provance, D.W., James, T.L., and Mercer, J.A. (2002). Melanophilin, the product of the leaden locus, is required for targeting of myosin-Va to melanosomes. Traffic *3,* 124–132.

Ramalho, J.S., Anders, R., Jaissle, G.B., Seeliger, M.W., Huxley, C., and Seabra, M.C. (2002). Rapid degradation of dominant-negative Rab27 proteins in vivo precludes their use in transgenic mouse models. BMC Chromatogr. Cell Biol. [serial online] *3,* 26. Available at www.biomedcentral.com.

Schlamp, C.L., and Williams, D.S. (1996). Myosin V in the retina: localization in the rod photoreceptor synapse. Exp. Eye Res. *63,* 613–619.

Seabra, M.C. (1996). New insights into the pathogenesis of choroideremia: a tale of two REPs. Ophthalmic Genet. *17,* 43–46.

Seabra, M.C., Ho, Y.K., and Anant, J.S. (1995). Deficient geranylgeranylation of Ram/Rab27 in choroideremia. J. Biol. Chem. *270,* 24420–24427.

Seabra, M.C., Mules, E.H., and Hume, A.N. (2002). Rab GTPases, intracellular traffic and disease. Trends Mol. Med. *8,* 23–30.

Self, T., Mahony, M., Fleming, J., Walsh, J., Brown, S.D., and Steel, K.P. (1998). Shaker-1 mutations reveal roles for myosin VIIA in both development and function of cochlear hair cells. Development *125,* 557–566.

Slot, J.W., Geuze, H.J., Gigengack, S., Lienhard, G.E., and James, D.E. (1991). Immuno-localization of the insulin regulatable glucose transporter in brown adipose tissue of the rat. J. Cell Biol. *113,* 123–135.

Strom, M., Hume, A.N., Tarafder, A.K., Barkagianni, E., and Seabra, M.C. (2002). A family of Rab27-binding proteins: melanophilin links Rab27a and myosin Va function in melanosome transport. J. Biol. Chem. *277,* 25423–25430.

Thumann, G., Bartz-Schmidt, K.U., Kociok, N., Heimann, K., and Schraemeyer, U. (1999). Ultimate fate of rod outer segments in the retinal pigment epithelium. Pigment Cell Res. *12,* 311–315.

Todorov, P.T., Hardisty, R.E., and Brown, S.D. (2001). Myosin VIIA is specifically associated with calmodulin and microtubule-associated protein-2B (MAP-2B). Biochem. J. *354,* 267–274.

Troutt, L.L., and Burnside, B. (1989). Role of microtubules in pigment granule migration in teleost retinal pigment epithelial cells. Exp. Eye Res. *48,* 433–443.

van den Hurk, J.A. *et al.* (1997). Molecular basis of choroideremia (CHM): mutations involving the Rab escort protein-1 (REP-1) gene. Hum. Mutat. *9,* 110–117.

Weil, D. *et al.* (1995). Defective myosin VIIA gene responsible for Usher syndrome type 1B. Nature *374,* 60–61.

Wilson, S.M. *et al.* (2000). A mutation in Rab27a causes the vesicle transport defects observed in ashen mice. Proc. Natl. Acad. Sci. USA *97,* 7933–7938.

Wu, X., Bowers, B., Rao, K., Wei, Q., and Hammer, J.A., 3rd. (1998). Visualization of melanosome dynamics within wild-type and dilute melanocytes suggests a paradigm for myosin V function in vivo. J. Cell Biol. *143,* 1899–1918.

Wu, X., Rao, K., Bowers, M.B., Copeland, N.G., Jenkins, N.A., and Hammer, J.A., 3rd. (2001). Rab27a enables myosin Va-dependent melanosome capture by recruiting the myosin to the organelle. J. Cell Sci. *114,* 1091–1100.

Wu, X.S., Rao, K., Zhang, H., Wang, F., Sellers, J.R., Matesic, L.E., Copeland, N.G., Jenkins, N.A., and Hammer, J.A., 3rd. (2002). Identification of an organelle receptor for myosin-Va. Nat. Cell Biol. *4,* 271–278.